Mechanism of Delayed Double Ionization in a Strong Laser Field

F. Mauger, A. Kamor, C. Chandre, and T. Uzer

Mechanism of delayed double ionization in a strong laser field

F. Mauger[1], A. Kamor[2], C. Chandre[1], T. Uzer[2]

[1] *Centre de Physique Théorique, CNRS – Aix-Marseille Université,*
Campus de Luminy, case 907, F-13288 Marseille cedex 09, France
[2] *School of Physics, Georgia Institute of Technology, Atlanta, GA 30332-0430, USA*

When intense laser pulses release electrons nonsequentially, the time delay between the last recollision and the subsequent ionization may last longer than what is expected from a direct impact scenario ["Recollision Excitation with Subsequent Ionization" (RESI)]. We show that the resulting delayed ionization stems from the inner electron being promoted to a sticky region. We identify the mechanism that traps and releases the electron from this region. As a signature of this mechanism, we predict oscillations in the ratio of RESI to double ionization yields versus laser intensity.

PACS numbers: 32.80.Rm, 05.45.Ac, 32.80.Fb

Atoms in strong laser pulses lose their electrons through two ionization channels [1]: A sequential one (SDI) and its non-sequential counterpart (NSDI). The SDI mechanism consists of successive and independent removals of the electrons. The recollision (or three-step) scenario [2, 3] in which a pre-ionized electron returns to the ion core to dislodge a bound electron is the characteristic mechanism for NSDI. It turns out that there is a rich variety of pathways among NSDI processes, also. At first sight, these pathways can be distinguished by the time it takes the second electron to ionize after the recollision. The common variant involves little, if any, delay between the recollision and ionization. However, this so-called "direct impact ionization" [4] is often accompanied by an alternative (and less straightforward) road to NSDI called Recollision Excitation with Subsequent Ionization (or RESI for short [4–12]). Recent experiments have shown that RESI can be the dominant channel for very short pulses [13]. The mechanism for RESI is often attributed to the recollision which excites the parent ion, later ionized by the laser field with a significant delay after the recollision (lasting from a quarter up to several laser cycles) and thereby imitating a sequential process.

The conventional picture for RESI involves the inner electron waiting passively for the pre-ionized electron to recollide, putting recollision as a central element in the excitation leading to the subsequent ionization. We revisit this picture by using a true nonsequential description of the process where both electrons interact with the laser field. We identify the mechanism that regulates the delayed subsequent ionization. Hitting the pool of available initial states (see cartoon in Fig. 1), a recollision may send the inner electron into the ionization continuum directly, thereby causing two electrons to emerge with very little time delay (direct impact ionization) or the recollision may drive the bound electron towards the parts of phase space which funnel electrons into the ionization continuum – which, given sufficient time, the electrons may have reached without the help of a recollision.

This common-sense distinction between the direct impact ionization and processes involving delayed double
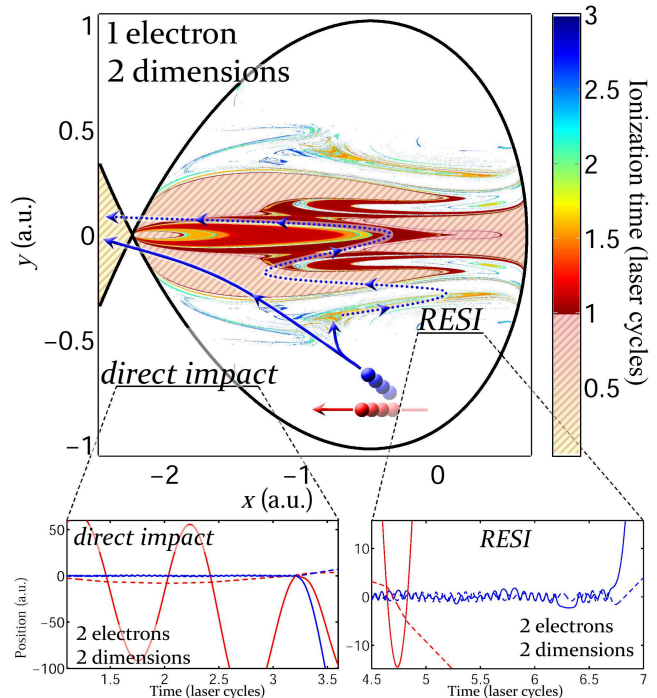

FIG. 1: Upper panel: Ionization time for Hamiltonian (2) with two dimensions for $I = 3 \times 10^{15}$ W · cm^{-2}, $\phi_0 = \pi/2$ and 780 nm. Initial conditions are chosen at the energy of the Stark saddle [14] with $p_x \leq 0$ and $p_y = 0$. After a recollision (full line arrows), the inner electron can be directly ionized or promoted to an excited state that is ionized with a delay (symbolized by dotted arrows). Lower panels: Typical two-electron trajectories for direct impact ionization (left) and RESI (right). Continuous (dashed) curves denote x (y) coordinates.

ionization, of which RESI is a prime example, emerges from our classical calculations [15] which allow both electrons to interact with each other and with the field and are, therefore, fully nonsequential. Our treatment confirms that the second ionization in delayed double ionization happens at the extrema of the laser field, in harmony with observations [4, 9, 16–18].

More generally, classical ensemble methods [19, 20]

have been remarkably successful in identifying direct impact ionization as well as RESI pathways that lead to double ionization and reproduce the experimental and computational observations closely. We consider a generic two active electron atom with soft-Coulomb potentials subjected to an intense and short linearly polarized laser pulse in the dipole approximation [15, 19–22]. The Hamiltonian is:

$$\mathcal{H}\left(\mathbf{x}_1, \mathbf{x}_2, \mathbf{p}_1, \mathbf{p}_2, t\right) = \frac{\|\mathbf{p}_1\|^2}{2} + \frac{\|\mathbf{p}_2\|^2}{2} - \frac{2}{\sqrt{\|\mathbf{x}_1\|^2 + a^2}}$$

$$- \frac{2}{\sqrt{\|\mathbf{x}_2\|^2 + a^2}} + \frac{1}{\sqrt{\|\mathbf{x}_1 - \mathbf{x}_2\|^2 + b^2}}$$

$$+ (\mathbf{x}_1 + \mathbf{x}_2) \cdot \mathbf{e}_x E_0 f(t) \sin \omega t, \qquad (1)$$

where $\mathbf{x}_i$ is the position vector of the ith electron in d dimensions and $\mathbf{p}_i$ is its canonically conjugate momentum. The linearly polarized (along the x-direction with unit vector $\mathbf{e}_x$) laser field is characterized by its amplitude E_0 and has a wavelength of 780 nm or 460 nm ($\omega = 0.0584$ or 0.1 a.u. respectively) with a shape $f(t)$ consisting of a two-cycle linear ramp-up and six laser cycle constant plateau. The constants a and b are the electron-nucleus and electron-electron softening parameters respectively chosen to be compatible with the ground state energy $\mathcal{E}_g$ (defined as the sum of the first and second ionization potentials). For the computations considered in this paper, we choose $a = b = 1$ and $\mathcal{E}_g = -2.3$ a.u. [15, 19–22], even though qualitatively similar results are observed with different parameters.

To begin with, we investigate the dynamics when both electrons are confined to a single dimension along the axis of polarization, i.e., $d = 1$. The motivation for studying the one-dimensional model is twofold: First, the laser field drives the dynamics along the polarization axis by which ionization is naturally expected to happen. Second, we find that this simplified dynamics forms the skeleton of higher-dimensional dynamics, which, however, differs from the single-dimensional dynamics in significant ways, to be specified below. It should be noted that three-dimensional calculations give similar results to two-dimensional ones due to the cylindrical symmetry of the problem around the polarization axis.

In what follows, delayed double ionizations refer to trajectories for which there is a long delay, compared to the direct impact scenario, between the last time the pre-ionized electron influences the core dynamics and the subsequent ionization. Among these delayed double ionizations, RESI events are described by two-electron trajectories for which, after a last recollision, one electron remains bound to the nucleus before ionizing. A recollision is said to have occurred whenever the distance between the two electrons is smaller than some threshold, which we set to 3.18 a.u for computations. We use an energy criterion to designate an electron as ionized
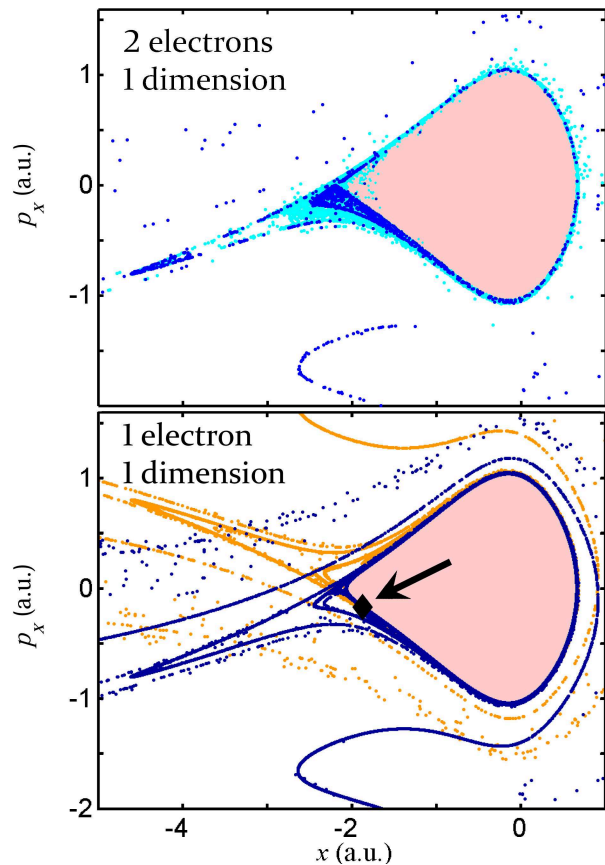

FIG. 2: Stroboscopic plots at the maxima of the laser field, for $I = 3 \times 10^{15}$ W · cm^{-2} and 780 nm during the plateau of the laser. Upper panel: detected RESI trajectories, after the last recollision, for Hamiltonian (1). Initial conditions are chosen as in Refs. [15, 23]. For each RESI, the first point on the section is plotted in light blue while the following ones are in dark blue. Lower panel: stable (light orange dots) and unstable (dark blue dots) manifolds of the periodic orbit $\mathcal{O}_{12}$ of Hamiltonian (2). The position of $\mathcal{O}_{12}$ is indicated with a black diamond (see the arrow). The pink area in the panels represents the part of phase space from which the inner electron does not ionize.

or not [15, 23], i.e., the kinetic plus Coulomb interaction with the core being positive. For the clarity of the illustrations we display RESIs with a time delay of at least two laser cycles between the last recollision and the ionization of the remaining ion. Qualitatively similar results are obtained with different (shorter or longer than the laser period) time delays. In Fig. 2 (upper panel), we display stroboscopic coordinate-momentum plots (taken at the maxima of the field) of detected RESIs. In what follows, we explain the rationale for these swirling patterns and connect them to full-dimensional calculations.

Delayed ionizations are best understood using a single electron model: The inner electron is in an excited state while the pre-ionized electron remains ionized. It allows us to neglect the electron-electron interaction in Hamiltonian (1) [15]. The resulting reduced-dimensional

Hamiltonian reads

$$\mathcal{H}(\mathbf{x}, \mathbf{p}, t) = \frac{\|\mathbf{p}\|^2}{2} - \frac{2}{\sqrt{\|\mathbf{x}\|^2 + a^2}}$$

$$+ \mathbf{x} \cdot \mathbf{e}_x E_0 \sin(\omega t + \phi_0), \tag{2}$$

where ϕ_0 denotes the phase at which the pre-ionized electron ceases to influence the core dynamics (e.g., after the final recollision).

The dynamics given by Hamiltonian (2) turns out to be the key to the patterns formed by the delayed ionized trajectories. Previous studies on Hamiltonian (2) [15, 23] with one spatial dimension have identified two qualitatively different kinds of dynamics for the electron driven by the field: In the competition between Coulomb attraction to the nucleus and the laser excitation, either the latter prevails, and the electron is quickly ionized; or the Coulomb attraction manages to maintain the electron trapped near the core [24]. Two areas in phase space emerge from this distinction: A bound region, close to the nucleus (pink area in Fig. 2), where the electron is trapped by the nucleus and cannot ionize; and an unbound region, further away (white area in the same panels), where the electron is quickly ionized by the laser. A more detailed study shows that the behavior in the unbound region is more complex than anticipated. This is readily apparent in the patterns seen in the unbound region in Fig. 2. A thin transition layer in the unbound region, and located in the area where the Coulomb attraction and the laser excitation compete equally, is responsible for delayed ionization. In practice, we show that this transition region is organized by the main resonances between the free field dynamics [$E_0 = 0$ in Hamiltonian (2)] and the laser (the electron oscillates exactly n times around the nucleus in one laser cycle, and we refer them as 1:n resonances). These resonances give birth to periodic orbits, among which at least one, denoted $\mathcal{O}_n$, is unstable (hyperbolic). Other periodic orbits in the vicinity of the bound region merely influence the fine details of the chaotic structure. Periodic orbits do not lead to ionization because they correspond to recurrent motions. However, neighboring trajectories may do so after some time, particularly if the periodic orbit is weakly unstable, as it is the case for selected periodic orbits $\mathcal{O}_n$. The pathways by which the electrons approach or leave the core are quantified by the so-called stable and unstable manifolds [25] around an unstable periodic orbit. In Fig. 2 (lower panel) we draw the stable and unstable manifolds of $\mathcal{O}_n$ (light orange and dark blue points respectively) for $n = 12$. Note the strong similarity between the unstable manifold and the Poincaré sections of RESI trajectories for the two-electron Hamiltonian (1) (upper panel). This similarity confirms the key role played by this one-electron unstable manifold in the delayed double ionization process. In addition, we see that the stable and unstable manifolds intersect an infinite number of times,
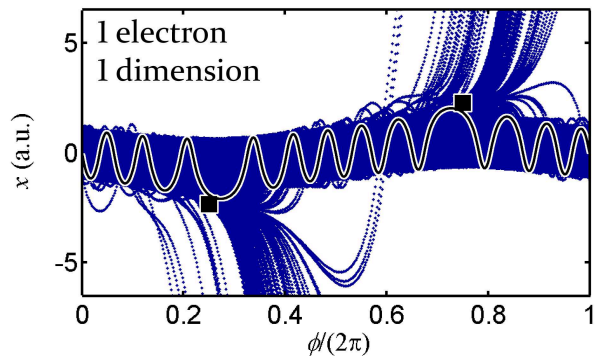

FIG. 3: Projection of the unstable manifold of the periodic orbit $\mathcal{O}_{12}$ of Hamiltonian (2) for $I = 3 \times 10^{15}$ W $\cdot$ cm^{-2} and 780 nm in the (x, ϕ) plane. The black curve is a projection of the periodic orbit in the plane (x, ϕ), and the black squares indicate the position of the saddle point at the extrema of the field.

a characteristic feature of a chaotic dynamics [26]. The overlap between the stable and unstable manifolds of $\mathcal{O}_n$ forms a "sticky" region [25] that traps trajectories for some time before ionizing. An electron promoted to this region can stay an arbitrary long time trapped in it, or not, depending on the position and momentum right after the promotion to the sticky region. The trapping time is typically long if the electron is promoted close to a periodic orbit, or short if it is further away, the distribution of trapping times being linked to the properties of the chaotic region. To better understand how delayed electrons find their way to ionization, we display a projection of the unstable manifold of $\mathcal{O}_n$ in the position–phase of the laser plane $(x, \phi = \omega t + \phi_0)$, together with a projection of $\mathcal{O}_n$ in Fig. 3. Two main branches depart from the central region near $x = 0$ when the laser phase is $\phi = \pi/2$ and $\phi = 3\pi/2$, i.e., near the extrema of the electric field, confirming that RESI takes place approximately at the extrema of the electric field [4, 17].

The organizing role of resonant periodic orbits can also be found in the relative proportion of RESI to double ionization yields: In Fig. 4, we compute this relative yield as the intensity is varied. It shows oscillations which are correlated with the intensity range where the 1:n resonance regulates the delayed ionization. The bound region (pink area in Fig. 2) shrinks with increasing laser intensity, and higher-order resonant periodic orbits are drawn to the unbound region. It means that as $\mathcal{O}_n$ becomes too unstable, the next resonance (associated with periodic orbit $\mathcal{O}_{n+1}$) is at play. Note the correlation between the oscillations and the stability index [25] of the resonant periodic orbits identified from the one-electron model (2). The stability index measures the typical time this orbit is expected to influence the neighboring dynamics: The larger the stability index, the sooner a neighboring trajectory diverges from it. Recent experimental results [27], with elliptic polarization, have revealed oscillations in the parallel to
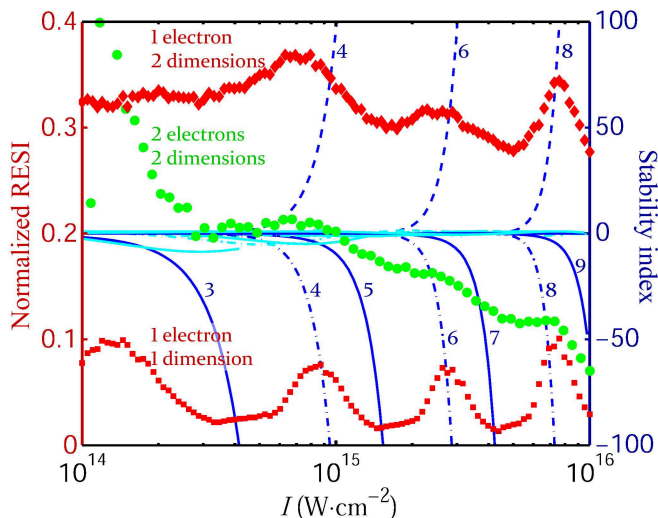
FIG. 4: Normalized RESI yields for 460 nm wavelength laser (markers, left hand y-axis). Red squares (diamonds) label one (two) dimensional one-electron simulations (normalized to the number of non-ionized trajectories). Green dots label two-dimensional two-electron simulations (normalized to the number of double ionization). While we show results for two laser cycle delays, qualitatively similar results are observed with shorter or longer delays. Curves label the linear stability index [25] of the resonant periodic orbits $\mathcal{O}_n$ of Hamiltonian (2) (curves, right hand y-axis) as functions of the laser intensity I. Continuous (broken) curves refer to odd (even) 1:n resonances. As intensity increases, the order of the resonance goes from $n = 3$ to $n = 9$ as indicated on the curves.

anti-parallel double ionization yields analogous to the oscillations observed in the RESI yields of Fig. 4.

Adding a dimension to the one-dimensional calculations provides more scope for the electron dynamics and makes the dynamics more complex. In particular, due to the extra dimension, the dynamics close to the nucleus region becomes partially chaotic both for one- and two-electron Hamiltonians (2) and (1) as it is already seen in Fig. 1. It becomes harder to define a bound and unbound region for the inner electron. More importantly, the aforementioned 1:n resonances generally enhance (linear) instability in the transverse direction while not affecting the organization of the dynamics in the (polarization) symmetry subspace: At a given intensity more than one resonance drives the delayed ionization dynamics in the sense that their unstable directions participate to the enhancement of delayed ionization. A direct consequence is the smoothing of the oscillations in Fig. 4 for 460 nm wavelength. Increasing the wavelength to 780 nm gives birth to more resonances with a more dense tangle of unstable manifolds so that the oscillations are completely washed out in two-dimensional models whether they are one- or two-electron models, as observed from our classical calculations. More generally, our analysis predicts that the aforementioned oscillations occur at short wavelengths (here 460 nm) and they are

washed out at longer ones (here 780 nm). In Fig. 4 we notice that the yields are higher for a two-dimensional model than for one dimension. We attribute these higher yields to the aforementioned chaotic dynamics coming from an increase of instability associated with additional resonances in the full-dimensional models. It underscores once more the pivotal role played by the inner electron dynamics [Hamiltonian (2), i.e., without recollision] in these delayed double ionizations.

To conclude, we have analyzed the ingredients of delayed double ionization: it is an inner-electron process driven by the laser field, facilitated (but not necessarily caused) by recollisions. While reduced one dimensional models are adequate for sequential and direct impact double ionization processes, higher-dimensional models are needed to portray the delayed ionization dynamics accurately.

[1] W. Becker and H. Rottke, Contemporary Physics **49**, 199 (2008).
[2] P. B. Corkum, Phys. Rev. Lett. **71**, 1994 (1993).
[3] K. J. Schafer, *et al.*, Phys. Rev. Lett. **70**, 1599 (1993).
[4] A. Rudenko, *et al.*, Phys. Rev. Lett. **93**, 253001 (2004).
[5] S. L. Haan, J. S. Van Dyke, and Z. S. Smith, Phys. Rev. Lett. **101**, 113001 (2008).
[6] S. L. Haan, *et al.*, Phys. Rev. A **81**, 023409 (2010).
[7] T. Shaaran, M. T. Nygren, and C. Figueira de Morisson Faria, Phys. Rev. A **81**, 063413 (2010).
[8] S. Baier, A. Becker, and L. Plaja, Phys. Rev. A **78**, 013409 (2008).
[9] B. Feuerstein, *et al.*, Phys. Rev. Lett. **87**, 043003 (2001).
[10] V. L. B. de Jesus, *et al.*, J. Elec. Spect. **141**, 127 (2004).
[11] V. L. B. de Jesus, *et al.*, J. Phys. B. **37**, L161 (2004).
[12] C. Figueira de Morisson Faria and X. Liu, J. Modern. Opt. **58**, 1076 (2011).
[13] N. Johnson, M. Kling and R. R. Jones (private communication).
[14] R. Blumel and W. P. Reinhardt, *Chaos in Atomic Physics* (Cambridge U. Press, 1997).
[15] F. Mauger, C. Chandre, and T. Uzer, Phys. Rev. Lett. **102**, 173002 (2009); J. Phys. B. **42**, 165602 (2009).
[16] T. Weber, *et al.*, Phys. Rev. Lett. **84**, 443 (2000).
[17] R. Moshammer, *et al.*, Phys. Rev. Lett. **84**, 447 (2000).
[18] C. Ruiz and A. Becker, New J. Phys. **10**, 025020 (2008).
[19] R. Panfili, J. H. Eberly and S. L. Haan, Opt. Express **8**, 431 (2001).
[20] P. J. Ho, *et al.*, Phys. Rev. Lett. **94**, 093002 (2005).
[21] J. Javanainen, J. H. Eberly, and Q. Su, Phys. Rev. A **38**, 3430 (1988).
[22] S. L. Haan, R. Grobe, and J. H. Eberly, Phys. Rev. A **50**, 378 (1994).

[23] F. Mauger, C. Chandre, and T. Uzer, Phys. Rev. Lett. **104**, 043005 (2010); Phys. Rev. A **81**, 063425 (2010).

[24] B. Hu, J. Liu, and S.-g. Chen, Phys. Lett. A **236**, 533 (1997).

[25] S. Wiggins, *Introduction to applied nonlinear dynamical systems and chaos* (Springer, 2003).

[26] K. A. Mitchell, Physica D **238**, 737 (2009).

[27] A. N. Pfeiffer, *et al.* New J. Phys. **13**, 093008 (2011).